Do cosmological data rule out $f(\mathcal{R})$ with $w \neq -1$?

Richard A. Battye,[*] Boris Bolliet,[†] and Francesco Pace[‡]
Jodrell Bank Centre for Astrophysics, School of Physics and Astronomy, The University of Manchester, Manchester M13 9PL, United Kingdom

(Received 22 December 2017; published 31 May 2018)

We review the equation of state (EoS) approach to dark sector perturbations and apply it to $f(\mathcal{R})$ gravity models of dark energy. We show that the EoS approach is numerically stable and use it to set observational constraints on designer models. Within the EoS approach we build an analytical understanding of the dynamics of cosmological perturbations for the designer class of $f(\mathcal{R})$ gravity models, characterized by the parameter B_0 and the background equation of state of dark energy w. When we use the Planck cosmic microwave background temperature anisotropy, polarization, and lensing data as well as the baryonic acoustic oscillation data from SDSS and WiggleZ, we find $B_0 < 0.006$ (95% C.L.) for the designer models with $w = -1$. Furthermore, we find $B_0 < 0.0045$ and $|w + 1| < 0.002$ (95% C.L.) for the designer models with $w \neq -1$. Previous analyses found similar results for designer and Hu-Sawicki $f(\mathcal{R})$ gravity models using the effective field theory approach [Raveri *et al.*, Phys. Rev. D **90**, 043513 (2014); Hu *et al.*, Mon. Not. R. Astron. Soc. **459**, 3880 (2016)]; therefore this hints for the fact that generic $f(\mathcal{R})$ models with $w \neq -1$ can be tightly constrained by current cosmological data, complementary to solar system tests [Brax *et al.*, Phys. Rev. D **78**, 104021 (2008); Faulkner *et al.*, Phys. Rev. D **76**, 063505 (2007)]. When compared to a wCDM fluid with the same sound speed, we find that the equation of state for $f(\mathcal{R})$ models is better constrained to be close to -1 by about an order of magnitude, due to the strong dependence of the perturbations on w.

DOI: 10.1103/PhysRevD.97.104070

I. INTRODUCTION

With the observational campaign of supernovae type Ia [1–4], followed by observations of the cosmic microwave background (CMB) anisotropy [5,6], the baryon acoustic oscillations (BAO) [7,8], and large scale structure [9–11], it has become widely accepted that the expansion of the universe is accelerating. The current observational data are consistent with the standard Λ cold dark matter (CDM) model, where the accelerated expansion is caused by the cosmological constant Λ, and indicate no statistically significant evidence for dark energy and modified gravity models (see, e.g., [12] and references therein).

Nevertheless, the cosmological constant suffers from important conceptual issues when it is interpreted in the context of quantum field theory (see, e.g., [13] for a recent review). This has led part of the community to question the physical origin of the accelerated expansion and to investigate dark energy and modified gravity models (see, e.g., [14]). Whether these models do not suffer the same type of issues as the cosmological constant often remains under debate.

Moreover, the forthcoming galaxy surveys and stage IV CMB experiments will measure the acceleration of the universe and its consequences on structure formation at a level of accuracy never achieved before. Hence, research on dark energy and modified gravity is well motivated by the following question: In the light of this forthcoming data, will the cosmological constant still be the best answer to cosmic acceleration? In other words, is there a modified gravity or dark energy model that will account for the observational data in a better way than the cosmological constant? Of course, this has to be formulated in a precise statistical manner; see [15] for an example in the context of inflationary models.

Recently, the Horndeski models [16–18] have received growing attention due to their generality. They include a scalar field coupled to gravity. The Horndeski Lagrangian is the most general one that leads to second order equations of motion for the scalar field. It is fully represented by four arbitrary time dependent functions of the scalar field and its kinetic term. Notable subclasses of the Horndeski models, obtained by specifying the unknown functions, are quintessence [19–26], k-essence [27–32], Brans-Dicke theory [33,34], kinetic gravity braiding (KGB) [35,36], and $f(\mathcal{R})$ models [37–40]. The latter can also be constructed by replacing the Ricci scalar $\mathcal{R}$ in the Einstein-Hilbert Lagrangian by an arbitrary function, $f(\mathcal{R})$, and are the main focus of this paper.

[*]richard.battye@manchester.ac.uk
[†]boris.bolliet@manchester.ac.uk
[‡]francesco.pace@manchester.ac.uk

Here, we are interested in $f(\mathcal{R})$ models that mimic the ΛCDM (or the wCDM) cosmological expansion history but differ at the level of the dynamics of cosmological perturbations. Different approaches have been developed to study the phenomenology of cosmological perturbations in dark energy and modified gravity in a unified way, with the ultimate objective of deriving observational constraints. These include the parametrized post-Friedmanian (PPF) approach [41–44], the equation of state for perturbations (EoS) approach [45–47] (see also [48] for an earlier and similar approach), the effective field theory (EFT) approach [49–53], and an alternative method [54]. They are in principle equivalent (see [55] for a numerical consistency analysis), although they differ with respect to the choices of the phenomenological parametrization of dark energy and modified gravity. So far, the EFT approach has been applied to generic Horndeski models [51,52], while the EoS approach has been applied specifically to quintessence, k-essence, and KGB models [47], $f(\mathcal{R})$ gravity [56], and generalized Einstein-Aether theories [57]. In this paper we use the EoS approach, for which the dark energy and modified gravity models are specified in terms of the anisotropic stress and pressure of the perturbed dark energy fluid.

The paper is organized as follows. In Sec. II we review the EoS approach and its numerical implementation in a Boltzmann code for arbitrary dark energy and modified gravity models. In Sec. III we recall the features of the designer $f(\mathcal{R})$ models that are relevant to our analysis. In Sec. IV we study the phenomenology of cosmological perturbations propagating in the dark energy fluid of the models with constant $w_{\rm de}$, numerically as well as analytically. In Sec. V we present the linear matter power spectrum, the CMB temperature angular anisotropy power spectrum, and the CMB power spectrum of the lensing potential, computed for several designer models, and we derive observational constraints on the free parameters of the designer models, i.e., $w_{\rm de}$ and B_0, from current CMB and BAO data. In Sec. VI we compare $f(\mathcal{R})$ and wCDM gravity models and their observational constraints. We discuss our results and conclude in Sec. VII. In Appendix we present a comparison between the perturbed equations of state obtained within the EoS [58] and EFT approaches [51,52].

Unless otherwise stated, we use $8\pi\mathcal{G} = 1$ throughout the paper.

II. NUMERICAL IMPLEMENTATION OF THE EQUATION OF STATE APPROACH

In the EoS approach, modifications to general relativity are written in the right-hand sides of the field equations. Then, they can be interpreted as a stress energy tensor, mapping any modified gravity theory to a corresponding dark energy fluid. More precisely, we have

$$G_{\mu\nu} = T_{\mu\nu} + D_{\mu\nu}, \tag{1}$$

where $G_{\mu\nu}$ is the Einstein tensor, $T_{\mu\nu}$ is the stress energy tensor of the matter components, i.e., baryonic matter, radiation, and dark matter, and $D_{\mu\nu}$ is the stress-energy tensor of the dark energy fluid. The background geometry is assumed to be isotropic and spatially flat, with a line element $ds^2 = -dt^2 + a^2\delta_{ij}dx^i dx^j$, where a is the scale factor and t is the cosmic time. Because of the Bianchi identities and the local conservation of energy for the matter components, the stress energy tensor of the dark sector is covariantly conserved,

$$\nabla^\mu D_{\mu\nu} = 0. \tag{2}$$

The linear perturbation of the conservation equations (2) yields the general relativistic version of the Euler and continuity equations for the velocity and density perturbation. They characterize the dynamics of cosmological perturbations and can be written in terms of a gauge invariant density perturbation, Δ, and a rescaled velocity perturbation, Θ. These two quantities are defined as

$$\Delta \equiv \delta + 3(1+w)H\theta, \qquad \Theta \equiv 3(1+w)H\theta, \tag{3}$$

where $w \equiv P/\rho$ is the background equation of state, ρ and P are the homogeneous density and pressure, $\delta\rho$ is the density perturbation, θ is the divergence of the velocity perturbation, and $H \equiv (d\ln a/dt)$ is the Hubble parameter.

The rescaled velocity perturbation, Θ, is not a gauge invariant quantity, in the sense that its value depends on the choice of the coordinate system; see, e.g., [59]. To see this, say that Θ is evaluated in the conformal Newtonian gauge (CNG), i.e., $\Theta^{\rm c} = \Theta$, where the superscript c indicates the CNG. Then the value of the rescaled velocity perturbation in the synchronous gauge (SG), $\Theta^{\rm s}$, is given, in Fourier space, by

$$\Theta^{\rm s} = \Theta^{\rm c} - 3(1+w)T, \tag{4}$$

with

$$T \equiv \begin{cases} (h' + 6\eta')/(2{\rm K}^2) & \text{in the SG,} \\ 0 & \text{in the CNG,} \end{cases} \tag{5}$$

where ${\rm K} \equiv k/(aH)$ and k is the wave number of the perturbation, h and η are the scalar metric perturbations in the SG, and a prime denotes a derivative with respect to $\ln a$. Since the SG is defined as the rest frame of the CDM fluid, we see that T is nothing other than the velocity perturbation of the CDM fluid evaluated in the CNG.

To work in a gauge invariant way, with respect to the synchronous and conformal Newtonian gauges, we can define a gauge invariant velocity perturbation as

$$\hat{\Theta} \equiv \Theta + 3(1+w)T. \tag{6}$$

In the same line of thought, using the variable T, the evolution equations for the gauge invariant density perturbation and rescaled velocity perturbation can be written in a way that is valid for both gauges [56]. These are the so-called *perturbed fluid equations* and are given by

$$\begin{aligned} \Delta' - 3w\Delta - 2\Pi + g_{\rm K}\epsilon_{\rm H}\hat{\Theta} &= 3(1+w)X, \\ \hat{\Theta}' + 3\left(c_{\rm a}^2 - w + \frac{1}{3}\epsilon_{\rm H}\right)\hat{\Theta} - 3c_{\rm a}^2\Delta - 2\Pi - 3\Gamma &= 3(1+w)Y, \end{aligned} \tag{7}$$

where $c_{\rm a}^2 \equiv dP/d\rho$ is the adiabatic sound speed and $g_{\rm K} \equiv 1 + {\rm K}^2/(3\epsilon_{\rm H})$, with $\epsilon_{\rm H} \equiv -H'/H$ and where

$$X \equiv \begin{cases} \eta' + \epsilon_{\rm H} T & \text{in the SG}, \\ \phi' + \psi & \text{in the CNG}, \end{cases} \tag{8a}$$

$$Y \equiv \begin{cases} T' + \epsilon_{\rm H} T & \text{in the SG}, \\ \psi & \text{in the CNG}. \end{cases} \tag{8b}$$

Finally, Π is the *perturbed scalar anisotropic stress*,[1] and Γ is the gauge invariant *entropy perturbation*. The gauge invariant entropy perturbation can be expressed in terms of the perturbed pressure, density, and rescaled velocity as

$$\Gamma = \frac{\delta P}{\rho} - c_{\rm a}^2(\Delta - \Theta). \tag{9}$$

The perturbed fluid equations (7) are valid for both matter (that we shall denote with a subscript "m") and dark energy (that we shall denote with subscript "de") fluid variables.

The Einstein-Boltzmann code `CLASS` [60,61] written in C provides the infrastructure required to solve the dynamics of matter perturbations. We have incorporated the EoS approach for dark energy perturbations into `CLASS` and dubbed the modified code `CLASS_EOS_FR`. The code is publicly available on the internet.[2] We have implemented the perturbed fluid equations (7) for dark energy perturbations in this exact same form. We now describe the remaining technical steps necessary to close the system of Eqs. (7) and integrate it in the code.

As prescribed by the EoS approach, we expand the perturbed dark energy anisotropic stress and gauge invariant entropy perturbation in terms of the perturbed fluid variables. These are the so-called *equations of state* for dark energy perturbations and are written as

$$\begin{aligned} \Pi_{\rm de} &= c_{\Pi\Delta_{\rm de}}\Delta_{\rm de} + c_{\Pi\Theta_{\rm de}}\hat{\Theta}_{\rm de} + c_{\Pi\Delta_{\rm m}}\Delta_{\rm m} + c_{\Pi\Theta_{\rm m}}\hat{\Theta}_{\rm m} + c_{\Pi\Pi_{\rm m}}\Pi_{\rm m}, \\ \Gamma_{\rm de} &= c_{\Gamma\Delta_{\rm de}}\Delta_{\rm de} + c_{\Gamma\Theta_{\rm de}}\hat{\Theta}_{\rm de} + c_{\Gamma\Delta_{\rm m}}\Delta_{\rm m} + c_{\Gamma\Theta_{\rm m}}\hat{\Theta}_{\rm m} + c_{\Gamma\Gamma_{\rm m}}\Gamma_{\rm m}, \end{aligned} \tag{10}$$

where the coefficients $c_{\alpha\beta}$ are *a priori* scale and time dependent functions, but shall only depend on the homogeneous background quantities, such as the Hubble parameter, the background equation of state of dark energy, or the adiabatic sound speeds. These functions are specified for each dark energy and modified gravity model; e.g., see [56] for $f(\mathcal{R})$ gravity and [57] for generalized Einstein-Aether. Note that the equations of state for perturbations for generic $f(\mathcal{R})$ models can also be obtained starting from a general Horndeski model and specifying the appropriate free functions to match with $f(\mathcal{R})$ theories. In this case, the expressions for the coefficients of $c_{\alpha\beta}$ are as reported in Appendix.

Initial conditions for dark sector perturbations are set at an early time, $a_{\rm ini}$, when dark energy is subdominant, i.e., $\Omega_{\rm de}(a_{\rm ini}) \ll 1$ where $\Omega_{\rm de}$ is the dark energy density parameter. If not specified from the specific dark energy model, appropriate initial conditions for the dark energy perturbations are generally $\Delta_{\rm de}(a_{\rm ini}) = \Theta_{\rm de}(a_{\rm ini}) = 0$. Note that when there exists an attractor for the dark energy perturbations during matter domination, it is numerically more efficient to set initial conditions that match the attractor (see Sec. IV).

In order to evaluate the equation of state (10) and integrate Eqs. (7), we collect the perturbed matter fluid variables at every time step. In our code, we do this in the following way. First, we obtain the total matter gauge invariant density perturbation via

$$\Omega_{\rm m}\Delta_{\rm m} = -\frac{2}{3}{\rm K}^2 Z - \Omega_{\rm de}\Delta_{\rm de} \quad \text{with} \quad Z \equiv \begin{cases} \eta - T & \text{in the SG} \\ \phi & \text{in the CNG} \end{cases} \tag{11}$$

and the gauge invariant matter velocity perturbation via $\Omega_{\rm m}\hat{\Theta}_{\rm m} = 2X - \Omega_{\rm de}\hat{\Theta}_{\rm de}$; see [56] where these equations are derived. Next, the matter pressure perturbation $\delta P_{\rm m}$ and the matter anisotropic stress $\sigma_{\rm m}^{\rm class}$ are available in `CLASS`. We use them to compute the matter anisotropic stress perturbation (in our convention) $\Pi_{\rm m}$ and the matter gauge invariant entropy perturbation as

$$\rho_{\rm m}\Pi_{\rm m} = -\frac{3}{2}\langle(\rho_{\rm m} + P_{\rm m})\sigma_{\rm m}^{\rm class}\rangle, \tag{12}$$

$$\rho_{\rm m}\Gamma_{\rm m} = \langle\delta P_{\rm m}\rangle - c_{a,{\rm m}}^2(\Delta_{\rm m} - \Theta_{\rm m}), \tag{13}$$

where the brackets mean a sum over *all* the matter fluid components, i.e., baryons, CDM, photons and neutrinos, and

$$c_{a,{\rm m}}^2 = \frac{w_{\rm m}\Omega_{\rm m} + \langle w_{\rm m}^2\Omega_{\rm m}\rangle}{(1+w_{\rm m})\Omega_{\rm m}} \tag{14}$$

[1]Note that our θ and Π differ from $\theta_{\rm MB}$ and $\sigma_{\rm MB}$ (anisotropic stress) as defined in [59], by $\theta_{\rm MB} = \frac{k^2}{a}\theta$ and $(\rho + P)\sigma_{\rm MB} = -\frac{2}{3}\rho\Pi$.

[2]Website: https://github.com/borisbolliet/class_eos_fr_public.

is the matter adiabatic sound speed, where $\Omega_m \equiv 1 - \Omega_{de}$ and $w_m \equiv \langle w_m \Omega_m \rangle / \Omega_m$ are the matter density parameter and background equation of state, respectively. Last, we update the total stress energy tensor accordingly as

$$\delta\rho_{tot} = \langle \delta\rho_m \rangle + \rho_{de}\Delta_{de} - \rho_{de}\Theta_{de},$$
$$(\rho_{tot} + P_{tot})\theta^{class}_{tot} = \langle (\rho_m + P_m)\theta^{class}_m \rangle + \frac{1}{3}K^2 aH\rho_{de}\Theta_{de},$$
$$(\rho_{tot} + P_{tot})\sigma^{class}_{tot} = \langle (\rho_m + P_m)\sigma^{class}_m \rangle - \frac{2}{3}\rho_{de}\Pi_{de},$$
$$\delta P_{tot} = \langle \delta P_m \rangle + \rho_{de}\Gamma_{de} + c^2_{a,de}\rho_{de}(\Delta_{de} - \Theta_{de}).$$

See footnote 1 for the CLASS perturbed velocity, which follows the conventions of [59].

Although the numerical integration can be carried out either in the conformal Newtonian gauge or in the synchronous gauge in CLASS_EOS_FR, we find that, in the super-Hubble regime, i.e., $K^2 \ll 1$, the synchronous gauge performs better than the conformal Newtonian gauge.

III. A BRIEF REMINDER ON THE DESIGNER $f(\mathcal{R})$ GRAVITY MODELS

In $f(\mathcal{R})$ gravity, the $f(\mathcal{R})$ functions are solutions to a second order differential equation given by the projection of the stress-energy tensor of $f(\mathcal{R})$ on the time direction, which can be written as [37,62–65]

$$f'' + \left(3\epsilon_H - 1 - \frac{\bar{\epsilon}'_H}{\bar{\epsilon}_H}\right)f' - \bar{\epsilon}_H f = 6H^2\bar{\epsilon}_H\Omega_{de}, \quad (15)$$

where the prime still denotes a derivative with respect to $\ln a$ and $\bar{\epsilon}_H = \epsilon'_H + 4\epsilon_H - 2\epsilon^2_H$ [see Eq. (2.6a) of [56] for the derivation in our conventions]. This equation holds for any $f(\mathcal{R})$ gravity model and at any time during the expansion history. During the nonrelativistic matter era, i.e., $w_m = 0$, this equation simplifies because $\epsilon_H = 3/2$, $\bar{\epsilon}'_H = 0$, and $\bar{\epsilon}_H = \epsilon_H = 3/2$ [see Eq. (2.5) of [56]]. In this regime, the solutions to (15) are

$$f(a) = C\left\{b_+ a^{n_+} + b_- a^{n_-} + e^{-\int 3(1+w_{de})\mathrm{d}\ln a}\right\}, \quad (16)$$

with $n_\pm = \frac{7}{4}(-1 \pm \sqrt{73/49})$ and $C = \frac{6\Omega^0_{de}H^2_0}{6w^2_{de}+5w_{de}-2}$. Solutions with $b_- \neq 0$ are not admissible because they break the condition $\lim_{a\to 0} f_{\mathcal{R}} = 0$ [66–68], where a subscript "$\mathcal{R}$" means a derivative with respect to the Ricci scalar. We conclude that any viable $f(\mathcal{R})$ gravity model can be parametrized, in the nonrelativistic matter era, by the *a priori* time dependent equation of state $w_{de}(a)$ and a constant number b_+. We then trade b_+ for the more commonly used parameter

$$B \equiv -\frac{f'_{\mathcal{R}}}{\epsilon_H(1 + f_{\mathcal{R}})}, \quad (17)$$

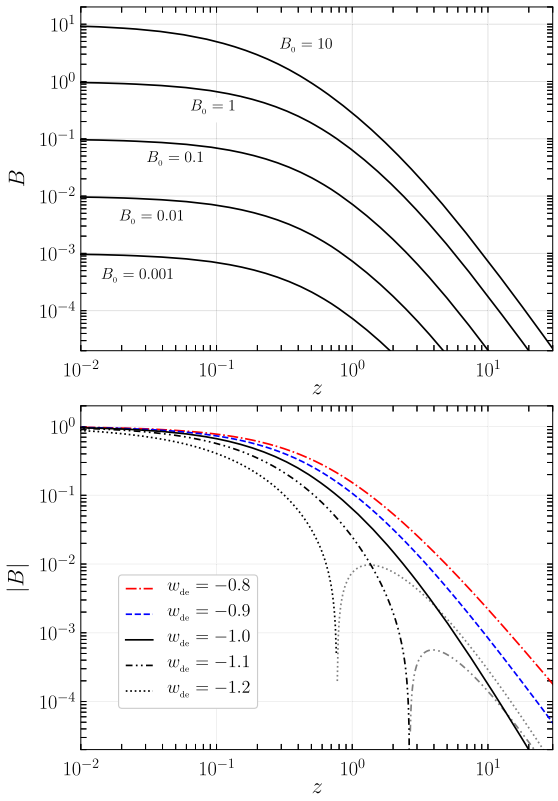

FIG. 1. The redshift evolution of $B = -(f'_{\mathcal{R}}/[\epsilon_H(1 + f_{\mathcal{R}})])$ for different designer $f(\mathcal{R})$ models. Unless otherwise written, we chose $w_{de} = -1$ and $B_0 = 1$. A grey line indicates negative values. The background cosmology was set to $h = 0.7, \Omega_{de} = 0.7$, and $\Omega_b h^2 = 0.022$, where $h = H_0/100$ is the reduced Hubble parameter.

evaluated today and dubbed B_0, since there is a one-to-one correspondence between b_+ and B_0. From here, there are two ways to proceed. The first possibility is to specify explicitly a $f(\mathcal{R})$ function at all time, and then extract the time evolution of Ω_{de} and w_{de} from the time derivatives of f. The second possibility is to specify a time evolution for Ω_{de} and w_{de} and then integrate Eq. (15) to get $f(\mathcal{R})$ at all time. This latter approach is the so-called designer, or mimetic, $f(\mathcal{R})$ approach and leads to the $f(\mathcal{R})$ gravity models that we are interested in. Designer models are particularly interesting because their functional form is dictated by the chosen background evolution of the dark fluid, and therefore there is no arbitrariness in how the $f(\mathcal{R})$ Lagrangian looks. In this way the wanted background evolution is achieved exactly and the model has fewer degrees of freedom: the only value to be determined is B_0, which ultimately will dictate the strength of the perturbations.

In CLASS_EOS_FR, we have implemented the designer models with constant equation of state w_{de}. The user specifies a value for w_{de} and B_0, and then the code explores a range of b_+ solving (15), between a_{ini} and today, until it finds the value of b_+ that leads to the desired value of B_0. Note that the solution in (16) is singular for $w_{de} \simeq 0.30$ and

$w_{de} \simeq -1.13$; however, as long as one avoids the two poles, the numerical integration is efficient.

In [37,56], the designer models with $w_{de} = -1$ were studied at both the background and the perturbation levels. Here, we consider as well the designer models with $w_{de} \neq -1$ (and $w'_{de} = 0$), i.e., the ones that mimic a wCDM expansion history.

In Fig. 1 we show the redshift evolution of a set of solutions to (15) for different values of B_0 and w_{de}. We present B, rather than $f(\mathcal{R})$ itself, because this is the main quantity entering the equations of state for perturbation Π_{de} and Γ_{de} [56]. On the bottom panel we fix $B_0 = 1$ and vary w_{de}. For models with $w_{de} < -1$, B starts being negative and eventually becomes positive at late time. This can be described analytically with Eq. (16); see, e.g., [37]. On the top panel we fix $w_{de} = -1$ and vary B_0. As can be seen, as soon as dark energy dominates, i.e., $z \lesssim 0.3$, B settles to its final value B_0. Changing the value of w_{de} essentially amounts to a shift of the curves on this plot because for a less negative w_{de} dark energy dominates earlier. The bottom panel shows that when we keep B_0 fixed, B grows more slowly for less negative w_{de}. More precisely, with Eq. (16) in the matter era, one finds $B \sim z^{3w_{de}}$.

IV. EVOLUTION OF PERTURBATIONS IN THE DARK ENERGY FLUID OF $f(\mathcal{R})$ GRAVITY

In this section we investigate numerically and analytically the evolution of cosmological perturbations for the designer $f(\mathcal{R})$ gravity models described in Sec. III. To this aim, we use the formalism of the EoS approach described in Sec. II.

To gain some understanding about the behavior of the cosmological perturbations, we consider the expressions of the equations of state for perturbations for a $f(\mathcal{R})$ fluid with constant equation of state parameter, i.e., $c^2_{a,de} = w_{de}$, and when the matter sector is dominated by nonrelativistic species, i.e., $w_m = \Pi_m = \Gamma_m = 0$, as is the case after radiation domination. Furthermore, we focus on modes that enter the Hubble horizon before dark energy dominates so that we have $K^2 \gg 1$ at all times. This assumption holds for wave numbers in the observational range of interest to us (see top panel of Fig. 2). Finally we assume $B \ll 1$, which is true at all times if $B_0 \ll 1$ and is equivalent to $M^2 \gg 1$, with $M^2 \equiv 2\bar{\epsilon}_H/(\epsilon_H B)$. In this regime, the equations of state for dark energy perturbations simplify to

$$\Pi_{de} = \Delta_{de}, \tag{18a}$$

$$\Gamma_{de} = \left\{\frac{1}{3} - w_{de} + \frac{M^2}{K^2}\right\}\Delta_{de} + \frac{1}{3}\frac{\Omega_m}{\Omega_{de}}\Delta_m. \tag{18b}$$

Using the field equations (3.11a) and (3.11b) in [56], the perturbed fluid equations (7) can be rewritten as a system of two coupled second order differential equations for the gauge invariant density perturbations,

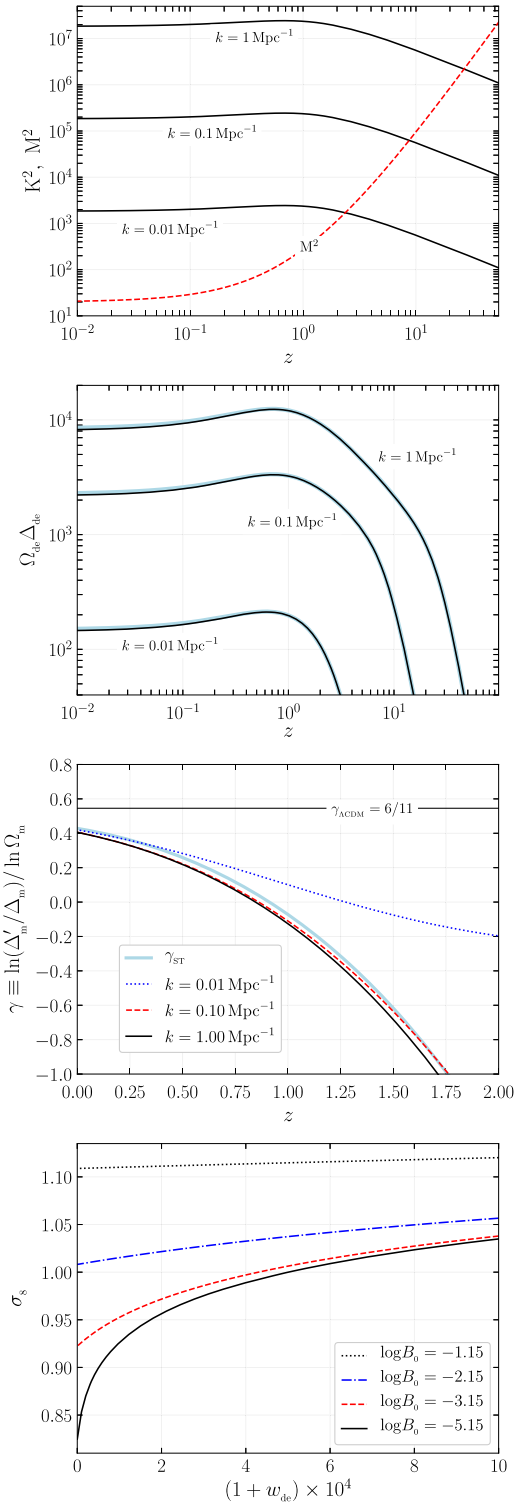

FIG. 2. The redshift evolution of K^2 for three wave numbers and M^2 (dashed line in the top panel), $\Omega_{de}\Delta_{de}$ and γ (middle panels), and σ_8 as a function of w_{de} (bottom panel) for different designer $f(\mathcal{R})$ models. The attractor solution (20) and the growth index γ_{ST} (25) are the thick grey lines. Unless otherwise written, we chose $w_{de} = -1$ and $B_0 = 0.1$ as well as the same cosmology as in Fig. 1 with $A_s = 2.2 \times 10^{-9}$ and $n_s = 0.96$.

$$\Delta_m'' + (2-\epsilon_H)\Delta_m' - \frac{3}{2}\Omega_m\Delta_m = -\frac{3}{2}\Omega_{de}\Delta_{de}, \quad (19a)$$

$$\Delta_{de}'' + (2-\epsilon_H)\Delta_{de}' + (K^2+M^2)\Delta_{de} = -\frac{1}{3}\frac{\Omega_m}{\Omega_{de}}K^2\Delta_m. \quad (19b)$$

For the modes of interest, this set of equations provides a faithful description of the dynamics of cosmological perturbations as long as $B \ll 1$. Again, this is always the case before dark energy dominates (irrespective of B_0). In addition, if $B_0 \ll 1$, then these equations are also valid during dark energy domination, because B is always smaller than B_0 (see Fig. 1). Let us assume $B_0 = \mathcal{O}(1)$, or equivalently $M^2 \gg 1$, from now on. As we shall see in Sec. V, this is a reasonable assumption given current observational constraints.

The differential equation (19b) for the gauge invariant energy density perturbation is similar to an harmonic oscillator with a time dependent frequency $\omega^2 = K^2 + M^2 \gg 1$. Since the oscillatory time scale is much smaller than the damping time scale, i.e., the expansion rate, the homogeneous solution to (19b) becomes rapidly subdominant compared to the particular solution. This confirms that the specific values for the initial dark energy perturbations are not important. More precisely, the dark energy density perturbation relates to the matter density perturbation via

$$\Omega_{de}\Delta_{de} = -\frac{1}{3}\frac{K^2}{K^2+M^2}\Omega_m\Delta_m. \quad (20)$$

We refer to [69] for the same result formulated in a different language. In our code, we set the initial conditions for Δ_{de} and Θ_{de} according to (20) at a time such that $K^2/[3(K^2+M^2)] = |\Omega_{de}\Delta_{de}/\Omega_m\Delta_m| = 0.01$. Note that given this criterion, the initial starting time for dark energy perturbation depends on the wave number.

We deduce from (20) the two regimes for the behavior of subhorizon modes: (i) the general relativistic (GR) regime when $K^2 \ll M^2$, i.e., at early time, and (ii) the scalar-tensor (ST) regime when $K^2 \gg M^2$, i.e., at late time. This implies $\Omega_{de}\Delta_{de} = -\frac{K^2}{M^2}\Omega_m\Delta_m$ in the GR regime, and $\Omega_{de}\Delta_{de} = -\frac{1}{3}\Omega_m\Delta_m$ in the ST regime. Moreover, in both regimes, the differential equation for the matter perturbation (19a) becomes

$$\Delta_m'' + (2-\epsilon_H)\Delta_m' - \frac{3}{2}\varepsilon\Omega_m\Delta_m = 0, \quad (21)$$

where $\varepsilon \equiv (4K^2+3M^2)/(3K^2+3M^2)$ can be interpreted as a *modification* to the gravitational constant [70]. One has $\varepsilon = 4/3$ in the ST regime and $\varepsilon = 1$ in the GR regime. Since one has $K^2 \sim z^{-1}$ and $M^2 \sim z^{-3w_{de}}$ during the matter era, the ST regime starts earlier for less negative w_{de}.

Equations (20) and (21) enable a clear discussion of the dynamics of cosmological perturbations in $f(\mathcal{R})$ gravity. Before doing so, we go one step further and obtain the growth index $\gamma \equiv \ln f/\ln\Omega_m$ of the matter perturbation [71], where $f \equiv \Delta_m'/\Delta_m$ is the growth rate.

Taking the time derivative of the growth rate and using (21) we find

$$\gamma' + \frac{3w_{de}\Omega_{de}}{\ln\Omega_m}\gamma + \frac{\Omega_m^\gamma}{\ln\Omega_m} - \frac{3\Omega_m^{1-\gamma}}{2\ln\Omega_m}\varepsilon = \frac{3w_{de}\Omega_{de}-1}{2\ln\Omega_m}, \quad (22)$$

for the growth index. To linearize this equation, we use the approximations $\ln\Omega_m \approx -\Omega_{de}$ and $\Omega_m^\gamma \approx 1-\gamma\Omega_{de}$, which are valid when $\Omega_{de} = \mathcal{O}(1)$. We get

$$\gamma' + \left(1 - 3w_{de} + \frac{3}{2}\varepsilon\right)\gamma = \frac{3}{2}\left(\frac{1-\varepsilon}{\Omega_{de}} + \varepsilon - w_{de}\right). \quad (23)$$

This can be solved analytically for a constant ε. We find

$$\gamma = \frac{3(1-\varepsilon)}{2+3\varepsilon}\frac{\Omega_{m,0}}{\Omega_{de,0}}(1+z)^{-3w_{de}} + \frac{3(\varepsilon-w_{de})}{2+3\varepsilon-6w_{de}}. \quad (24)$$

In the GR regime the first term on the right-hand side vanishes, and the second term gives a constant $\gamma_{w\mathrm{CDM}} = 3(1-w_{de})/(5-6w_{de})$, i.e., the wCDM growth index. If in addition $w_{de} = -1$, the growth index is $\gamma_{\Lambda\mathrm{CDM}} = 6/11 \approx 0.545$, i.e., the well-known ΛCDM result. In the ST regime, the growth index is not constant any more due to the first term on the right-hand side. We find

$$\gamma_{ST} = \frac{1}{2} + \frac{1}{6(1-w_{de})} - \frac{\Omega_{m,0}}{6\Omega_{de,0}}(1+z)^{-3w_{de}}. \quad (25)$$

Since the first term on the right-hand side of (24) is always negative, we have $\gamma_{ST} < \gamma_{w\mathrm{CDM}}$ as well as $\gamma_{ST} < \gamma_{\Lambda\mathrm{CDM}}$.

We now summarize the important consequences for the dynamics of perturbations in $f(\mathcal{R})$ gravity that are deduced from the above considerations.

(1) For $B < 0$ (or $M^2 < 0$), the homogeneous solution to (19b) is unstable. Therefore, the gauge invariant density perturbation for both matter and dark energy grows exponentially with time. This is not compatible with the dynamics of matter perturbations in the matter dominated era, and consequently $f(\mathcal{R})$ models with $B_0 < 0$ or $w_{de} < -1$ are not viable; see Fig. 1.

(2) The gauge invariant density perturbation in the dark energy component relates to that of the matter component in a simple way given in (20). In the GR regime, the dark energy perturbation is negligible compared to the matter perturbation, while in the ST regime both are of the same magnitude; see Fig. 2.

(3) In wCDM, for less negative w_{de} structures are less gravitationally bounded compared to ΛCDM because dark energy starts dominating earlier. Hence

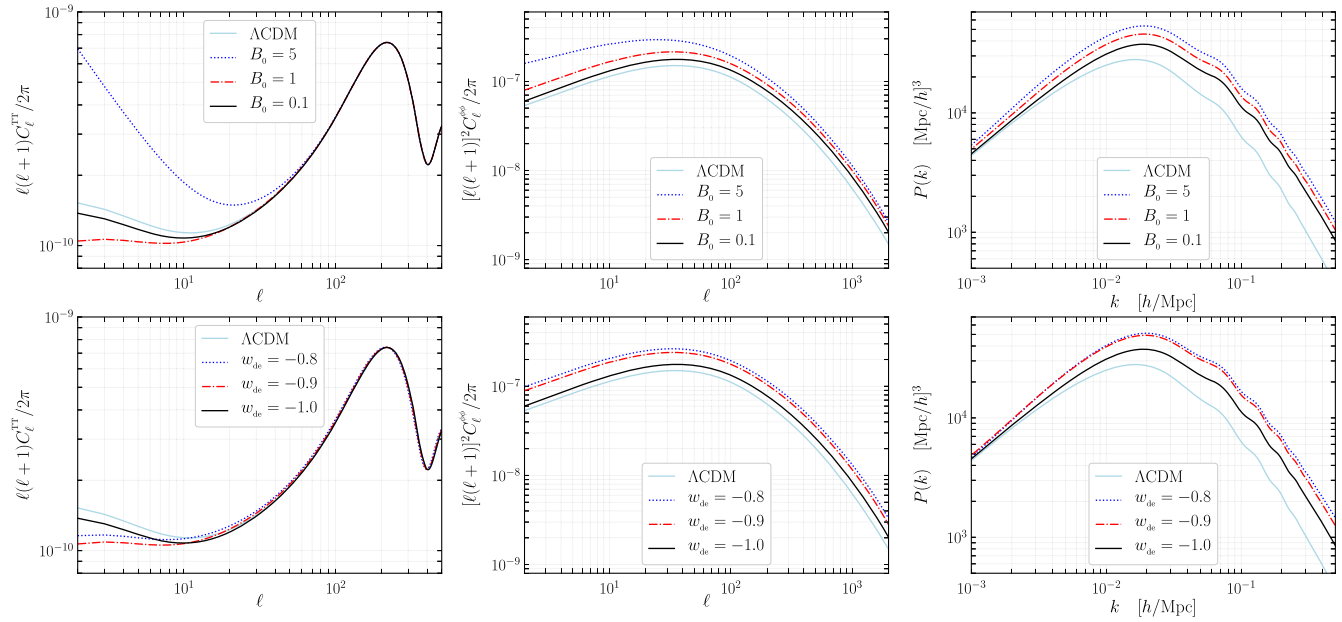

FIG. 3. Effects of $f_{\mathcal{R}}$ gravity on the CMB angular temperature power spectrum (left), the lensing power spectrum (middle), and the linear matter power spectrum (right) for different designer $f(\mathcal{R})$ models against the ΛCDM predictions. Unless otherwise written, we chose $w_{\rm de} = -1$ and $B_0 = 0.1$ as well as the same cosmology as in Fig. 2.

there is an *anticorrelation* between $w_{\rm de}$ and the amplitude of clustering, i.e., σ_8, in wCDM models (see, e.g., Fig. 16 of [72]). In $f(\mathcal{R})$ gravity matter perturbations grow at a faster rate than in wCDM and ΛCDM because $\gamma_{\rm ST} < \gamma_{w\rm CDM}$ [see Eq. (25)]. This, combined with the fact that the ST regime starts earlier for less negative $w_{\rm de}$, implies a *correlation* between $w_{\rm de}$ and σ_8 (see bottom panel of Fig. 2), and can be used to discriminate between $f(\mathcal{R})$ gravity and wCDM models of dark energy [see also the next section for a comparison between wCDM and $f(\mathcal{R})$ models].

In the next section we compute relevant observables that we use to set observational constraints on the designer $f(\mathcal{R})$ gravity models.

V. IMPACT OF $f(\mathcal{R})$ GRAVITY ON OBSERVABLES AND CONSTRAINTS

The CMB angular anisotropy power spectrum is a snapshot of the acoustic waves in the photon-baryon fluid at decoupling, distorted by the integrated Sachs-Wolfe effect (ISW) and the lensing due to the subsequent gravitational collapse of the matter. How and when can dark energy perturbations in $f(\mathcal{R})$ gravity affect the CMB anisotropy? Since in viable $f(\mathcal{R})$ gravity models dark energy perturbations are subdominant at early time (see point 2 above), they cannot have any impact on the physical phenomena at play at the epoch of decoupling. However, they alter the growth of structure from the end of the matter dominated era (see point 3 above). Therefore, they may have an impact on the *late* ISW effect (see, e.g., [73]) and lensing of the CMB anisotropy (see, e.g., [74]). The late ISW effect is contributing to the CMB temperature anisotropy on large angular scales ($\ell \lesssim 20$) and the lensing power spectrum of the CMB probes structure formation on a wider range of scales ($\ell \lesssim 1000$). So we expect the CMB angular anisotropy power spectrum to be affected by dark energy perturbations only at low multipoles, i.e., where the cosmic variance limits the constraining power of the CMB data. Hence, the lensing power spectrum shall be a more compelling probe of dark energy perturbation than the CMB temperature anisotropy angular power spectrum.

In the left panels of Fig. 3 we show the CMB temperature angular anisotropy power spectrum computed for several designer models with different $w_{\rm de}$ and B_0, against the ΛCDM prediction. We see that significant differences appear when $B_0 \gtrsim 1$ and that the late ISW effect can be strongly enhanced for larger values of B_0. Moreover, at fixed B_0 the late ISW contribution is more significant for less negative $w_{\rm de}$, as can be understood with the results of Sec. IV (see point 3 above). In the middle panels we show the CMB lensing power spectrum computed in the same settings. Its amplitude is larger for larger B_0 and less negative $w_{\rm de}$, again in agreement with the analysis of Sec. IV. Similar conclusions apply to the linear matter power spectrum presented in the right panels of Fig. 3. In particular, for scales that are still in the GR regime today ($k \approx 10^{-3} h$ Mpc^{-1}), the amplitude of the matter power spectrum is close to the ΛCDM prediction, while for scales that entered the ST regime during the matter dominated era ($k \gtrsim 10^{-2} h$ Mpc^{-1}), its amplitude is enhanced.

TABLE I. Posterior mean (68% C.L.) for $\log B_0$, σ_8, and w_{de} for designer $f(\mathcal{R})$ models that mimic a ΛCDM and a wCDM expansion. The ellipses indicate the absence of 68% C.L. constraints; in this case only the 95% C.L. upper limits are relevant (see Table II).

	CMB + BAO (ΛCDM)	CMB + BAO + lensing (ΛCDM)	CMB + BAO (wCDM)	CMB + BAO + lensing (wCDM)
$\log B_0$	$-2.01^{+1.26}_{-0.19}$	...	...	...
σ_8	$1.04^{+0.10}_{-0.03}$	...	$1.13^{+0.05}_{-0.03}$	$0.98^{+0.05}_{-0.03}$
$(1+w_{de})\times 10^3$	0	0	$8.10^{+1.50}_{-8.10}$	$0.64^{+0.08}_{-0.64}$

TABLE II. Posterior upper limits (95% C.L.) for $\log B_0$, σ_8, and w_{de} for designer $f(\mathcal{R})$ models that mimic a ΛCDM and a wCDM expansion.

	CMB + BAO (ΛCDM)	CMB + BAO + lensing (ΛCDM)	CMB + BAO (wCDM)	CMB + BAO + lensing (wCDM)
$\log B_0$	<-0.78	<-2.2	<-1.26	<-2.35
σ_8	<1.13	<0.99	<1.18	<1.04
$(1+w_{de})\times 10^3$	0	0	<20	<2.1

For observational constraints, we consider the following combinations of data sets: CMB + BAO and CMB, BAO + lensing. For CMB and lensing we refer to the Planck 2015 public likelihoods for low-ℓ and high-ℓ temperatures as well as polarization and lensing data [5]. For BAO we refer to the distance measurements provided by the WiggleZ Dark Energy Survey [75] and SDSS [76]. We use `Montepython` [77] for the Monte Carlo Markov chain sampling of the parameter space. We varied the six base cosmological parameters as well as all the Planck nuisance parameters. For those, we used the same priors as the Planck Collaboration [5]. In addition, we varied the background dark energy equation of state w_{de} and $\log B_0$ that characterize the designer $f(\mathcal{R})$ models. For w_{de} we used a uniform prior between -1 and 0. For $\log B_0$ we used a uniform prior between -6 and 1. In Tables I and II, we show the 68% C.L. and 95% C.L. constraints from our analyses.

For designer models with $w_{de}=-1$, B_0 and σ_8 are determined at 68% C.L. for CMB + BAO. We get $B_0 \approx 0.01$ and $\sigma_8 \simeq 1.0 \pm 0.1$. If we add the information relative to clustering at late time, via the CMB lensing data, B_0 and σ_8 are not determined, but constrained to $B_0 \lesssim 0.006$ and $\sigma_8 < 1.0$ (95% C.L.).

For designer models with $w_{de} \neq -1$, B_0 is not determined any more by CMB + BAO. Moreover, because of the correlation between w_{de} and the amplitude of clustering (see bottom panel of Fig. 2), σ_8 takes substantially larger values than with the $w_{de}=-1$ models. When we add CMB lensing data, the posterior mean value of σ_8 is brought down by 15% and more importantly the 68% C.L. region for the dark energy background equation of state is reduced by a factor of 10. We get $(1+w_{de}) < 0.0006$; in other words, the expansion history has to be very close to ΛCDM.

VI. COMPARISON WITH wCDM MODELS

To quantify the relative importance of perturbations in (designer) $f(\mathcal{R})$ models, we can compare their observational constraints with a wCDM model where the background equation of state w is free to vary (but constant in time) and we keep the sound speed (defined in the frame comoving with the fluid) $c_s^2 = \delta p/\delta\rho = 1$ fixed. To study the perturbations of such a model, we use the `CLASS` implementation of the PPF framework as described in [78]. When $w_{de} \geq -1$, this framework recovers the behavior of canonical minimally coupled scalar field models, and it is accurate also when $w_{de} \approx -1$. A welcome aspect of the PPF formalism is that it allows one to study the evolution of perturbations in the phantom regime ($w_{de} < -1$), which is usually preferred by supernovae data [3,79]. In addition, the crossing of the "phantom barrier" ($w_{de} = -1$) is allowed, covering therefore also the more general case of non-canonical minimally coupled models, such as k-essence. The PPF formalism allows also sound speeds $c_s^2 \neq 1$, as in k-essence models, but here we limit ourselves to the standard case of luminal sound speed, as this is also the value in $f(\mathcal{R})$ models.

We note, in principle, that in wCDM models w_{de} can take values smaller than -1 (this is the so-called phantom regime), while in the designer $f(\mathcal{R})$ models we consider in this work the phantom crossing is not allowed due to instabilities (see Sec. IV).

Moreover, we saw that in $f(\mathcal{R})$ gravity small variations of w_{de} lead to large variations in σ_8 (see bottom panel of Fig. 2), while in wCDM models small variations of w_{de} lead to small variations in σ_8: in the range of w_{de} presented in the bottom panel of Fig. 2, for the same cosmological parameters, σ_8 would vary by less than 1%.

TABLE III. Posterior mean (68% C.L.) for σ_8 and w_{de} for a wCDM model.

	CMB + BAO	CMB + BAO + lensing
σ_8	$0.85^{+0.02}_{-0.02}$	$0.83^{+0.02}_{-0.02}$
$(1+w_{de})\times 10^2$	$-7.35^{+7.76}_{-5.9}$	$-4.7^{+6.5}_{-6.1}$

TABLE IV. Posterior upper limits (95% C.L.) for σ_8 and w_{de} for a wCDM model.

	CMB + BAO	CMB + BAO + lensing
σ_8	<0.89	<0.87
$(1+w_{de})\times 10^2$	<5.9	<8

Using the same data sets described before, in Tables III and IV we show the 68% C.L. and 95% C.L. constraints on σ_8 and w_{de} for the wCDM fluid, respectively. For w_{de}, we use a uniform prior between -2 and 0.

Our results agree with [5]. In particular, the preferred value for w_{de} is in the phantom regime. It means that these data sets favor a higher value of σ_8 with respect to the ΛCDM cosmology, as was the case for the $f(\mathcal{R})$ models.

Our last remark is that since σ_8 depends weakly on w_{de} in wCDM compared to $f(\mathcal{R})$, the constraints on w_{de} in wCDM are weaker than in $f(\mathcal{R})$ by 1 order of magnitude (see Tables III and IV).

VII. DISCUSSION AND CONCLUSION

Intense observational and theoretical efforts are being deployed to unveil the nature of the cosmic acceleration of the universe. Going beyond the cosmological constant Λ, two main hypotheses can be explored: dark energy and modified gravity. Many models belonging to these two broad groups can be described in terms of the Horndeski Lagrangian. In this work we concentrated on a well studied subclass of Horndeski theories, the so-called $f(\mathcal{R})$ gravity models. Such modifications to GR may affect both the background expansion history and the evolution of cosmological perturbations. In this paper we considered the designer $f(\mathcal{R})$ gravity models for which the $f(\mathcal{R})$ function is tuned to reproduce the wCDM expansion history.

We used the EoS approach to study analytically the dynamics of linear cosmological perturbations in this context, and we implemented it numerically in our `CLASS_EOS_FR` code. To prove the reliability of our numerical implementation, we compared our results with several other $f(\mathcal{R})$ codes publicly available such as `MGCAMB` [80,81], `FRCAMB` [82], `EFTCAMB` [83–85] and found agreement at the subpercent level for all of them [55], except for `MGCAMB` which disagreed by more than 5% relative error with the other codes for the computation of the matter power spectrum for $k > 1h$ Mpc^{-1}.

Unlike for the simple wCDM dark energy model, we found that for designer $f(\mathcal{R})$ gravity models a less negative w_{de} leads to a larger σ_8 (see point 3 above). To arrive at this conclusion we derived an analytical formula for the growth index γ [see Eq. (25)].

Using CMB lensing data we found that designer $f(\mathcal{R})$ models with $(1+w_{de}) > 0.002$ and $B_0 > 0.006$ are disfavored at 95% C.L. Note that similar constraints were obtained for the designer $f(\mathcal{R})$ models also by [83], using cosmological data as we did here. The authors of [86] performed a similar analysis on the Hu-Sawicki $f(\mathcal{R})$ models and found, as we did, a higher value of σ_8 with respect to the ΛCDM value.[3] Moreover, for the screening mechanism to happen on solar system scales the authors of [88,89] found $|1+w_{de}| \lesssim 10^{-4}$ for generic $f(\mathcal{R})$ models.

The results we obtained are consistent with these previous analyses and hint for the fact that generic $f(\mathcal{R})$ models with $w_{de} \neq -1$ can be ruled out based on current cosmological data, complementary to solar system tests.

ACKNOWLEDGMENTS

We thank Ruth Durrer, Marco Raveri, Alessandra Silvestri, Filippo Vernizzi, Bin Hu, Jens Chluba, and Lucas Lombriser for discussions. We thank Julien Lesgourgues, Thomas Tram, and Thejs Brinckmann for their help with CLASS and Montepython. F. P. acknowledges financial support from the STFC Grant No. R120562. B. B. acknowledges financial support from the ERC Consolidator Grant No. 725456. Part of the analysis presented here is based on observations obtained with Planck (http://www.esa.int/Planck), an ESA science mission with instruments and contributions directly funded by ESA Member States, NASA, and Canada. We also thank the referee whose comments helped us to improve the scientific content of this work.

APPENDIX: COMPARISON BETWEEN THE EOS AND EFT APPROACHES FOR DARK ENERGY PERTURBATIONS

In this section we compare the expressions for the entropy perturbations and the perturbed anisotropic stress of [56] with the corresponding expressions from [52] in the conformal Newtonian gauge. In the following we will denote with the superscript "BBP" variables in [56] and with "GLV" variables in [52]. In addition, we use the subscript "m" for all matter species and

$$\zeta_i = \frac{g_K \epsilon_H - \bar{\epsilon}_H}{3 g_K \epsilon_H} - \frac{dP_i}{d\rho_i}. \tag{A1}$$

[3]Using CFHTLenS data [87], the normalization of the matter power spectrum is significantly closer to the ΛCDM value, implying a lower value of $f_{\mathcal{R},0}$ (B_0 in our notation) and, using their Eq. (10) (see also their Fig. 2), $w_{de} \approx -1$.

In $f(\mathcal{R})$ gravity the equations of states for scalar perturbations, in both formalisms are [52,56]

$$\Pi_{\rm de}^{\rm BBP} = \frac{\mathrm{K}^2}{3g_{\rm K}\epsilon_{\rm H}}\left\{\Delta_{\rm de} - \frac{f'_{\mathcal{R}}}{2(1+f_{\mathcal{R}})}\Theta_{\rm de} + \frac{\Omega_{\rm m}}{\Omega_{\rm de}}\frac{f_{\mathcal{R}}}{1+f_{\mathcal{R}}}\Delta_{\rm m} - \frac{\Omega_{\rm m}}{\Omega_{\rm de}}\frac{f'_{\mathcal{R}}}{2(1+f_{\mathcal{R}})}\Theta_{\rm m}\right\} - \frac{f_{\mathcal{R}}}{1+f_{\mathcal{R}}}\frac{\Omega_{\rm m}}{\Omega_{\rm de}}\Pi_{\rm m}, \tag{A2a}$$

$$\Gamma_{\rm de}^{\rm BBP} = \left\{\zeta_{\rm de} - \frac{\bar{\epsilon}_{\rm H}}{3g_{\rm K}\epsilon_{\rm H}}\frac{2(1+f_{\mathcal{R}})-f'_{\mathcal{R}}}{f'_{\mathcal{R}}}\right\}\Delta_{\rm de} - \zeta_{\rm de}\Theta_{\rm de} + \frac{\Omega_{\rm m}}{\Omega_{\rm de}}\left\{\zeta_{\rm m} - \frac{\bar{\epsilon}_{\rm H}}{3g_{\rm K}\epsilon_{\rm H}}\frac{2f_{\mathcal{R}}-f'_{\mathcal{R}}}{f'_{\mathcal{R}}}\right\}\Delta_{\rm m} - \frac{\Omega_{\rm m}}{\Omega_{\rm de}}\zeta_{\rm m}\Theta_{\rm m} - \frac{\Omega_{\rm m}}{\Omega_{\rm de}}\Gamma_{\rm m}, \tag{A2b}$$

$$P_{\rm de}^{\rm GLV}\Gamma_{\rm de}^{\rm GLV} = \frac{\gamma_1\gamma_2 + \gamma_3\alpha_{\rm B}^2\mathrm{K}^2}{\gamma_1 + \alpha_{\rm B}^2\mathrm{K}^2}(\delta\rho_{\rm de} - 3Hq_{\rm de}) + \frac{\gamma_1\gamma_4 + \alpha_{\rm B}^2\mathrm{K}^2}{\gamma_1 + \alpha_{\rm B}^2\mathrm{K}^2}H(q_{\rm de}+q_{\rm m}) + \frac{1}{3}(\delta\rho_{\rm m} - 3Hq_{\rm m}) - \frac{dP_{\rm de}}{d\rho_{\rm de}}\delta\rho_{\rm de} - \delta p_{\rm m}, \tag{A2c}$$

$$P_{\rm de}^{\rm GLV}\Pi_{\rm de}^{\rm GLV} = \frac{\gamma_8\alpha_{\rm B}^2\mathrm{K}^2}{2(\gamma_1 + \alpha_{\rm B}^2\mathrm{K}^2)}(\delta\rho_{\rm de} - 3Hq_{\rm de}) - \frac{\gamma_9\mathrm{K}^2}{2(\gamma_1 + \alpha_{\rm B}^2\mathrm{K}^2)}H(q_{\rm de}+q_{\rm m}), \tag{A2d}$$

where the functions γ_i are given by $\gamma_1 = 3\alpha_{\rm B}^2\epsilon_{\rm H}$, $\gamma_3 = \frac{1}{3}$, $\gamma_2 = \frac{1}{3} - \frac{\bar{\epsilon}_{\rm H}}{3\epsilon_{\rm H}\alpha_{\rm B}}$, $\gamma_4 = 1 - \frac{\bar{\epsilon}_{\rm H}}{\epsilon_{\rm H}}$, $\gamma_8 = -2$, and $\gamma_9 = -6\alpha_{\rm B}^3$. We further define $\alpha_{\rm B} = \frac{f'_{\mathcal{R}}}{2(1+f_{\mathcal{R}})}$. Note that with respect to [52], we defined $P_{\rm de}\Pi_{\rm de}^{\rm GLV} = -\frac{k^2}{a^2}\sigma_{\rm de}^{\rm GLV}$.

Unlike [58], the authors of [52] use a nonstandard continuity equation for the effective dark energy fluid, which implies

$$\rho_{\rm de}^{\rm GLV} = \rho_{\rm de}^{\rm BBP} + 3M_{\rm pl}^2H^2f_{\mathcal{R}},$$
$$P_{\rm de}^{\rm GLV} = P_{\rm de}^{\rm BBP} - M_{\rm pl}^2H^2(3-2\epsilon_{\rm H})f_{\mathcal{R}},$$

for the background and

$$\delta\rho_{\rm de}^{\rm GLV} = (1+f_{\mathcal{R}})\delta\rho_{\rm de}^{\rm BBP} + f_{\mathcal{R}}\delta\rho_{\rm m}^{\rm BBP},$$
$$\delta P_{\rm de}^{\rm GLV} = (1+f_{\mathcal{R}})\delta P_{\rm de}^{\rm BBP} + f_{\mathcal{R}}\delta P_{\rm m}^{\rm BBP},$$
$$q_{\rm m}^{\rm GLV} + q_{\rm de}^{\rm GLV} = -\frac{1+f_{\mathcal{R}}}{3H}\{\rho_{\rm de}^{\rm BBP}\Theta_{\rm de}^{\rm BBP} + \rho_{\rm m}^{\rm BBP}\Theta_{\rm m}^{\rm BBP}\},$$
$$q_{\rm de}^{\rm GLV} = -\frac{1}{3H}\{(1+f_{\mathcal{R}})\rho_{\rm de}^{\rm BBP}\Theta_{\rm de}^{\rm BBP} + f_{\mathcal{R}}\rho_{\rm m}^{\rm BBP}\Theta_{\rm m}^{\rm BBP}\},$$
$$P_{\rm de}^{\rm GLV}\Pi_{\rm de}^{\rm GLV} = [(1+f_{\mathcal{R}})P_{\rm de}^{\rm BBP}\Pi_{\rm de}^{\rm BBP} + f_{\mathcal{R}}P_{\rm m}^{\rm BBP}\Pi_{\rm m}^{\rm BBP}],$$

for the perturbed fluid variables. From this, we conclude that both formalisms are equivalent.

[1] A. G. Riess *et al.*, Astrophys. J. **116**, 1009 (1998).
[2] S. Perlmutter *et al.*, Astrophys. J. **517**, 565 (1999).
[3] A. G. Riess *et al.*, Astrophys. J. **607**, 665 (2004).
[4] A. G. Riess *et al.*, Astrophys. J. **659**, 98 (2007).
[5] Planck Collaboration XIII, Astron. Astrophys. **594**, A13 (2016).
[6] G. Hinshaw *et al.*, Astrophys. J. Suppl. Ser. **208**, 19 (2013).
[7] W. J. Percival *et al.*, Mon. Not. R. Astron. Soc. **401**, 2148 (2010).
[8] D. Parkinson *et al.*, Phys. Rev. D **86**, 103518 (2012).
[9] S. Alam *et al.*, Mon. Not. R. Astron. Soc. **470**, 2617 (2017).
[10] S. Rota *et al.*, Astron. Astrophys. **601**, A144 (2017).
[11] M. Ata *et al.*, Mon. Not. R. Astron. Soc. **473**, 4773 (2018).
[12] Planck Collaboration XIV, Astron. Astrophys. **594**, A14 (2016).
[13] D. H. Weinberg, M. J. Mortonson, D. J. Eisenstein, C. Hirata, A. G. Riess, and E. Rozo, Phys. Rep. **530**, 87 (2013).
[14] T. Clifton, P. G. Ferreira, A. Padilla, and C. Skordis, Phys. Rep. **513**, 1 (2012).
[15] T. Giannantonio and E. Komatsu, Phys. Rev. D **91**, 023506 (2015).
[16] G. W. Horndeski, Int. J. Theor. Phys. **10**, 363 (1974).
[17] C. Deffayet, X. Gao, D. A. Steer, and G. Zahariade, Phys. Rev. D **84**, 064039 (2011).
[18] T. Kobayashi, M. Yamaguchi, and J. Yokoyama, Prog. Theor. Phys. **126**, 511 (2011).
[19] L. H. Ford, Phys. Rev. D **35**, 2339 (1987).
[20] P. J. E. Peebles and B. Ratra, Astrophys. J. Lett. **325**, L17 (1988).
[21] B. Ratra and P. J. E. Peebles, Phys. Rev. D **37**, 3406 (1988).
[22] C. Wetterich, Nucl. Phys. **B302**, 668 (1988).

[23] R. R. Caldwell, R. Dave, and P. J. Steinhardt, Phys. Rev. Lett. **80**, 1582 (1998).
[24] E. J. Copeland, A. R. Liddle, and D. Wands, Phys. Rev. D **57**, 4686 (1998).
[25] P. J. Steinhardt, L. Wang, and I. Zlatev, Phys. Rev. D **59**, 123504 (1999).
[26] T. Barreiro, E. J. Copeland, and N. J. Nunes, Phys. Rev. D **61**, 127301 (2000).
[27] C. Armendáriz-Picón, T. Damour, and V. Mukhanov, Phys. Lett. B **458**, 209 (1999).
[28] T. Chiba, T. Okabe, and M. Yamaguchi, Phys. Rev. D **62**, 023511 (2000).
[29] N. A. Hamed, H. S. Cheng, M. A. Luty, and S. Mukohyama, J. High Energy Phys. 05 (2004) 074.
[30] F. Piazza and S. Tsujikawa, J. Cosmol. Astropart. Phys. 07 (2004) 004.
[31] R. J. Scherrer, Phys. Rev. Lett. **93**, 011301 (2004).
[32] V. Mukhanov and A. Vikman, J. Cosmol. Astropart. Phys. 02 (2006) 004.
[33] C. Brans and R. H. Dicke, Phys. Rev. **124**, 925 (1961).
[34] A. De Felice and S. Tsujikawa, J. Cosmol. Astropart. Phys. 07 (2010) 024.
[35] C. Deffayet, O. Pujolàs, I. Sawicki, and A. Vikman, J. Cosmol. Astropart. Phys. 10 (2010) 026.
[36] O. Pujolàs, I. Sawicki, and A. Vikman, J. High Energy Phys. 11 (2011) 156.
[37] Y.-S. Song, W. Hu, and I. Sawicki, Phys. Rev. D **75**, 044004 (2007).
[38] A. Silvestri and M. Trodden, Rep. Prog. Phys. **72**, 096901 (2009).
[39] T. P. Sotiriou and V. Faraoni, Rev. Mod. Phys. **82**, 451 (2010).
[40] A. De Felice and S. Tsujikawa, Living Rev. Relativity **13**, 3 (2010).
[41] C. Skordis, Phys. Rev. D **79**, 123527 (2009).
[42] T. Baker, P. G. Ferreira, C. Skordis, and J. Zuntz, Phys. Rev. D **84**, 124018 (2011).
[43] T. Baker, P. G. Ferreira, and C. Skordis, Phys. Rev. D **87**, 024015 (2013).
[44] P. G. Ferreira, T. Baker, and C. Skordis, Gen. Relativ. Gravit. **46**, 1788 (2014).
[45] R. A. Battye and J. A. Pearson, J. Cosmol. Astropart. Phys. 07 (2012) 019.
[46] R. A. Battye and J. A. Pearson, Phys. Rev. D **88**, 061301 (2013).
[47] R. A. Battye and J. A. Pearson, J. Cosmol. Astropart. Phys. 03 (2014) 051.
[48] M. Kunz and D. Sapone, Phys. Rev. Lett. **98**, 121301 (2007).
[49] J. Bloomfield, É. É. Flanagan, M. Park, and S. Watson, J. Cosmol. Astropart. Phys. 08 (2013) 010.
[50] J. Bloomfield, J. Cosmol. Astropart. Phys. 12 (2013) 044.
[51] J. Gleyzes, D. Langlois, F. Piazza, and F. Vernizzi, J. Cosmol. Astropart. Phys. 08 (2013) 025.
[52] J. Gleyzes, D. Langlois, and F. Vernizzi, Int. J. Mod. Phys. D **23**, 1443010 (2014).
[53] J. Gleyzes, D. Langlois, M. Mancarella, and F. Vernizzi, J. Cosmol. Astropart. Phys. 08 (2015) 054.
[54] D. Bertacca, N. Bartolo, and S. Matarrese, J. Cosmol. Astropart. Phys. 08 (2012) 021.
[55] E. Bellini *et al.*, Phys. Rev. D **97**, 023520 (2018).
[56] R. A. Battye, B. Bolliet, and J. A. Pearson, Phys. Rev. D **93**, 044026 (2016).
[57] R. A. Battye, F. Pace, and D. Trinh, Phys. Rev. D **96**, 064041 (2017).
[58] R. A. Battye and F. Pace, Phys. Rev. D **94**, 063513 (2016).
[59] C.-P. Ma and E. Bertschinger, Astrophys. J. **455**, 7 (1995).
[60] J. Lesgourgues, arXiv:1104.2932.
[61] D. Blas, J. Lesgourgues, and T. Tram, J. Cosmol. Astropart. Phys. 07 (2011) 034.
[62] L. Pogosian and A. Silvestri, Phys. Rev. D **77**, 023503 (2008).
[63] S. Nojiri, S. D. Odintsov, and D. Sáez-Gómez, Phys. Lett. B **681**, 74 (2009).
[64] P. K. S. Dunsby, E. Elizalde, R. Goswami, S. Odintsov, and D. Saez-Gomez, Phys. Rev. D **82**, 023519 (2010).
[65] L. Lombriser, A. Slosar, U. Seljak, and W. Hu, Phys. Rev. D **85**, 124038 (2012).
[66] J. Khoury and A. Weltman, Phys. Rev. D **69**, 044026 (2004).
[67] J. Khoury and A. Weltman, Phys. Rev. Lett. **93**, 171104 (2004).
[68] W. Hu and I. Sawicki, Phys. Rev. D **76**, 064004 (2007).
[69] S. Tsujikawa, R. Gannouji, B. Moraes, and D. Polarski, Phys. Rev. D **80**, 084044 (2009).
[70] A. A. Starobinsky and Sov, J. Exp. Theor. Phys. Lett. **86**, 157 (2007).
[71] P. J. E. Peebles, *The Large-Scale Structure of the Universe* (Princeton University Press, Princeton, NJ, 1980).
[72] E. Komatsu *et al.*, Astrophys. J. Suppl. Ser. **180**, 330 (2009).
[73] J. Lesgourgues, arXiv:1302.4640.
[74] A. Lewis and A. Challinor, Phys. Rep. **429**, 1 (2006).
[75] E. A. Kazin *et al.*, Mon. Not. R. Astron. Soc. **441**, 3524 (2014).
[76] A. J. Ross, L. Samushia, C. Howlett, W. J. Percival, A. Burden, and M. Manera, Mon. Not. R. Astron. Soc. **449**, 835 (2015).
[77] B. Audren, J. Lesgourgues, K. Benabed, and S. Prunet, J. Cosmol. Astropart. Phys. 02 (2013) 001.
[78] W. Fang, W. Hu, and A. Lewis, Phys. Rev. D **78**, 087303 (2008).
[79] J. L. Tonry *et al.*, Astrophys. J. **594**, 1 (2003).
[80] G.-B. Zhao, L. Pogosian, A. Silvestri, and J. Zylberberg, Phys. Rev. D **79**, 083513 (2009).
[81] A. Hojjati, L. Pogosian, and G.-B. Zhao, J. Cosmol. Astropart. Phys. 08 (2011) 005.
[82] J.-h. He, Phys. Rev. D **86**, 103505 (2012).
[83] M. Raveri, B. Hu, N. Frusciante, and A. Silvestri, Phys. Rev. D **90**, 043513 (2014).
[84] B. Hu, M. Raveri, N. Frusciante, and A. Silvestri, Phys. Rev. D **89**, 103530 (2014).
[85] B. Hu, M. Raveri, N. Frusciante, and A. Silvestri, arXiv:1405.3590.
[86] B. Hu, M. Raveri, M. Rizzato, and A. Silvestri, Mon. Not. R. Astron. Soc. **459**, 3880 (2016).
[87] C. Heymans *et al.*, Mon. Not. R. Astron. Soc. **432**, 2433 (2013).
[88] P. Brax, C. van de Bruck, A.-C. Davis, and D. J. Shaw, Phys. Rev. D **78**, 104021 (2008).
[89] T. Faulkner, M. Tegmark, E. F. Bunn, and Y. Mao, Phys. Rev. D **76**, 063505 (2007).